Error Performance of RIS-Assisted NOMA Networks with Imperfect Channel State Information

G. Cao[1], M. Li[1*], H. Yuan[2], W Chen[3] , L. Li[1] and A. Raouf[4]

[1] School of Electronics Information Engineering, Taiyuan University of Science and Technology, China.
[2] School of Computer Science and Mathematics, Kingston University, KT1 2EE, UK.
[3] Department of Electronic Engineering, Tsinghua University, China.
[4] Faculty of Technology at UISTAM, Abidjan.

Abstract—This paper investigates the impact of imperfect channel state information (ipCSI) on the performance of RIS-assisted NOMA vehicular networks while considering the effect of imperfect successive interference cancellation (ipSIC). Moreover, we present novel closed-form pairwise error probability (PEP) expressions with arbitrary L users. The PEP is used to evaluate the union bound on the bit error rate of NOMA users. Finally, the analysis is supported by numerical and Monte Carlo simulation results. We show that the impact of ipCSI with ipSIC on each user's error rate performance is great at the high P_s. We also confirm that the error rate performance of the system decreases with the increase of RUs.

Index Terms—Imperfect channel state information, imperfect successive interference cancellation, NOMA, RIS, pairwise error probability.

I. INTRODUCTION

It is envisioned that Vehicle-to-everything (V2X) will play an important role in autonomous driving as the sixth generation (6G) of wireless networks evolves. While V2X is designed to provide traffic-efficient message transmission in certain circumstances, a substantial volume of sensed data from vehicles must be transferred to infrastructure or other vehicles. As a result, the essential topic is maintaining continuous and reliable communication in a moving environment [1]. Meeting the stringent requirements for low latency and high reliability (LLHR) required for the V2X services is challenging.

In recent years, reconfigurable intelligent surfaces (RIS) have attracted attention. Deploying RISs can enhance the links without line-of-sight (LoS) propagation [2]. The benefits introduced by RIS hold great promise for the advanced V2X applications specified [3]. For massive and ubiquitous vehicular access, non-orthogonal multiple access (NOMA) has emerged as a promising wireless paradigm. NOMA techniques were proposed to allow various users simultaneously access the network at the same time and frequency band by using non-orthogonal resources, such as different power levels or low-density spreading codes, to improve spectrum efficiency and reduce the access latency [4].

Furthermore, non-ideal wireless communication characteristics, including imperfect successive interference cancellation (ipSIC) and imperfect channel status information (ipCSI), should be considered when evaluating system performance. As for the ipSIC implementation, there has been extensive research on how it affects the system performance for NOMA transmission [5], [6]. Secondly, especially in V2X communications, due to the mobility of vehicles and complicated cross-interference caused by the dense topology, perfect CSI is challenging for the BS to obtain in a mobile environment, which means that channel estimation errors may exist during the channel estimation process [7], [8].

However, the above papers mainly studied the system's outage probability, ergodic capacities and energy efficiency. Since BER analysis with ipSIC is intractable, the pairwise error probability (PEP) as the union bound of bit error rate (BER) can evaluate the error performance of the system well, which gained more attention [9]. To the best of the authors' knowledge, the only relevant papers on the PEP performance of RIS-assisted NOMA system have been reported in [10], [11], in which the authors investigated the error probability performance of RIS-assisted NOMA system. However, the authors didn't consider the impact of ipCSI with ipSIC.

Motivated by the above discussion, in this article, we investigate the effect of ipCSI on the PEP performance of a RIS-assisted NOMA system with ipSIC. Notably, we derive closed-form PEP expressions under the particular two scenarios. Further, the PEP performance is analysed for arbitrary L users, which is then utilized to obtain a union bound on the error rate.

The rest of this article is arranged as follows. Section II describes the considered system model. Section III takes the PEP as the performance index to evaluate the influence of imperfect CSI on the downlink RIS-NOMA system. In Section IV, numerical results are given to prove the correctness of the analysis. Ultimately, Section V is the conclusion.

Notation: $(\cdot)^*$ and $|\cdot|$ denote the complex conjugate operation and the absolute value, respectively. $\mathrm{Re}\,\{Z\}$ represents the real part of the complex number Z. $\|x\|_2^2$ denotes 2-norm of vector x.

II. SYSTEM MODEL

This article considers a downlink RIS-assisted NOMA system consisting of one base station (BS), one RIS consisting of N RUs, and L single-antenna users. The BS transmits the superimposed symbols $x_s = \sum_{l=1}^{L} \sqrt{\omega_l P_s} x_l$ to each vehicle, where P_s is the total transmitted signal power, ω_l is the l-th sorted power allocation coefficient with $\sum_{l=1}^{L} \omega_l = 1$, and

x_l is the transmitted symbol for U_l. Due to long-distance or major obstacles, we presume there is no direct connection between the BS and the vehicles. Without loss of generality, we assume that large-scale fading is dominant, and hence, channel qualities are determined based on the users' distances from the RIS. Then we consider the first vehicle has the weakest channel gain while the L-th vehicle has the strongest, i.e., $|g_{id1}|^2 < |g_{id2}|^2 < ... < |g_{idL}|^2$, and all the channels follow independent Rayleigh fading. Subsequently, the first user is allocated the highest power coefficient, while the L-th user is assigned the lowest power coefficient, i.e., $\omega_1 > \omega_2 > \cdots > \omega_l$. According to the principle of NOMA, U_l will utilize SIC technique to detect and subtract the signals of weaker users, i.e., $x_1, ..., x_{l-1}$, whilst treating the signals of stronger users, i.e., $x_{l+1}, ..., x_L$ as additive noise. However, in actual scenarios, detection errors may occur during the process of SIC, which results in imperfect SIC. Accordingly, the output signal of the $l - 1$ SIC process can be expressed as:

$$\hat{y}_l = \frac{\left(\sum_{i=1}^{N} h_{si} r_i g_{idl} + e_l \right)}{\sqrt{d_B^\alpha d_{R,l}^\alpha}} \left(\sqrt{\omega_l P_s} x_l + \sqrt{P_s} \theta_l \right) + n_l, \quad (1)$$

$\theta_l = \sum_{n=1}^{l-1} \sqrt{\omega_n} \Delta_n + \sum_{s=l+1}^{L} \sqrt{\omega_s} x_s$, where d_B is the reference distance between BS and RIS, and $d_{R,l}$ as the distance between the RIS and the l-th vehicle. Further, α as the pass-loss exponent, $r_i = \beta_i exp(j\phi_i)$ is the response of the i-th RU, and the reflection coefficients of phase shift and amplitude of the i-th RU are represented by ϕ_i and β_i respectively. Without loss of generality, we assume that $\beta_i = 1$. Moreover, e_l represents the channel estimation error which can be modelled as a complex Gaussian random variable (CGRV) with $e_l \sim \mathcal{CN}(0, \sigma_{e_l}^2)$, where $\sigma_{e_l}^2 = \delta^2 \left\| vec \left(\sum_{i=1}^{N} h_{si} r_i g_{idl} \right) \right\|_2^2$, $\delta \in [0,1)$, which represents the relative amount of CSI uncertainties. $\Delta_n = x_n - \hat{x}_n$ is the difference between the transmitted and detected signals of the l-th vehicle and $\sum_{n=1}^{l-1} \sqrt{\omega_n} \Delta_n$ represents the interference due to the ipSIC from users $U_1, ..., U_{l-1}$. $n_l \sim \mathcal{CN}(0, \sigma_n^2)$ denotes the additive white Gaussian noise (AWGN).

We focus on the error transmission performance, so we consider the case where the detected signals $\hat{x}_n$ are not equal to x_n in the following. We assume that RIS are completely aware of the phase $\phi_{h_{si}}$ of $BS \rightarrow RIS$ channel h_{si} and the phase $\phi_{g_{idl}}$ of $RIS \rightarrow U_l$ channel g_{idl}, and choose the best phase shift, i.e. $\phi_i = -(\phi_{h_{si}} + \phi_{g_{idl}})$.

The received signal of U_l can be rewritten as

$$\hat{y}_l = \underbrace{\frac{1}{\sqrt{d_B^\alpha d_{R,l}^\alpha}} q_l \sqrt{\omega_l P_s} x_l}_{\triangleq \text{desired information signal}} + \underbrace{\frac{1}{\sqrt{d_B^\alpha d_{R,l}^\alpha}} q_l \sqrt{P_s} \theta_l}_{\triangleq \text{SIC noise}}$$
$$\underbrace{+ \underbrace{\frac{1}{\sqrt{d_B^\alpha d_{R,l}^\alpha}} e_l \sqrt{P_s} \left(\sqrt{\omega_l} x_l + \theta_l \right)}_{\triangleq \text{ipCSI noise}} + \underbrace{n_l}_{\triangleq \text{white noise}}}_{}. \quad (2)$$

where $q_l = \sum_{i=1}^{N} |h_{si}| |g_{idl}|$ is the estimated channel coefficient.

Based on the considered system model, there are four scenarios, namely 1) pCSI and pSIC; 2) pCSI and ipSIC; 3) ipCSI and pSIC; 4) ipCSI and ipSIC. As for the first and the third scenarios, we only need to set $\Delta_n = 0$, which results in $\theta_l = \sum_{s=l+1}^{L} \sqrt{\omega_s} x_s$ for all users in (3). In the sequel, we focus mainly on the PEP performance analysis for the ipSIC assumption under both ipCSI (i.e., scenario 2) and pCSI cases (i.e., scenario 4).

III. PEP ANALYSIS

In this section, we derive an accurate expression for the PEP, defined as the probability of detecting symbol $\hat{x}$ given that symbol x was transmitted, where $\hat{x} \neq x$. As a result of the maximum-likelihood rule, the conditional PEP of the l-th user on the channel fading coefficient q_l may be evaluated as $\text{PEP}(x_l, \hat{x}_l | q_l) = \text{Pr}(g(\hat{x}_l) \leq g(x_l))$,

where

$$g(y) = \left| \hat{y}_l - \frac{1}{\sqrt{d_B^\alpha d_{R,l}^\alpha}} q_l \sqrt{\omega_l P_s} y \right|^2. \quad (3)$$

By substituting (2) into (3), one obtains

$$\text{PEP}(x_l, \hat{x}_l | q_l) = \text{Pr}\left(\mathcal{N} \leq \frac{1}{\sqrt{d_B^\alpha d_{R,l}^\alpha}} q_l^2 \sqrt{P_s} \widetilde{\xi}_l \right), \quad (4)$$

where $\widetilde{\xi}_l = -\sqrt{\omega_l} |\Delta_l|^2 - 2\text{Re}\{\Delta_l \theta_l^*\}$
and

$$\mathcal{N} = 2\text{Re}\left\{ \frac{q_l \Delta_l}{\sqrt{d_B^\alpha d_{R,l}^\alpha}} \left(\frac{e_l \sqrt{P_s}(\sqrt{\omega_l} x_l + \theta_l)}{\sqrt{d_B^\alpha d_{R,l}^\alpha}} + n_l \right)^* \right\}. \quad (5)$$

Further, $\mathcal{N}$ can be modelled by a Gaussian RV with zero mean and variance $\sigma_{\mathcal{N}}^2$ with

$$\sigma_{\mathcal{N}}^2 = \frac{4q_l^2 |\Delta_l|^2}{d_B^\alpha d_{R,l}^\alpha} \left(\frac{\left(w_l x_l^2 + |\theta_l|^2 \right)}{d_B^\alpha d_{R,l}^\alpha} \sigma_{e_l}^2 P_s + \sigma_n^2 \right). \quad (6)$$

Further, (4) can be evaluated by

$$\text{PEP}(x_l, \hat{x}_l | q_l) = Q\left(\frac{q_l \xi_l \sqrt{\bar{\gamma}_l}}{2|\Delta_l| \sqrt{\psi_l \bar{\gamma}_l + d_B^\alpha d_{R,l}^\alpha}} \right). \quad (7)$$

where $\xi_l = -\widetilde{\xi}_l$, $\psi_l = \sigma_{e_l}^2 \left(\omega_l x_l^2 + |\theta_l|^2 \right)$ and $\bar{\gamma}_l = \frac{P_s}{\sigma_n^2}$, $Q(\cdot)$ is the Gaussian Q-function [12, eq. (6.287.3)].

Remark 1:

- For U_2 and U_3, according to NOMA decoding rules, they must decode the high-power signal first and then their own signal. In the case of ipSIC, the decoding error will make θ_l larger, thus making ψ_l and ξ_l in (7) large, but due to the numerator goes up faster than the denominator, so that the overall value in Q function will become larger. Moreover, since the Q function is a monotone decreasing function, the PEP of the formula (7) will become smaller. That is, the PEPs of U_2 and U_3 under the ipSIC condition are significantly lower than that under the pSIC condition.

$$\text{PEP}\left(x_l, \hat{x}_l\right) = \frac{A\Theta_l}{b^{a+1}\left[\Gamma\left(a+1\right)\right]^{l+k}} \sum_{k=0}^{L-l} \binom{L-l}{k}(-1)^k \left(\sum_{n=0}^{\infty} c_n \mathcal{F}_l\right). \tag{13}$$

$$\mathcal{F}_l = \frac{1}{2\sqrt{\pi}}\left(\frac{\sqrt{2}}{\varepsilon_l}\right)^{a_l+1} \times H_{2,2}^{1,2}\left(\left.\frac{\sqrt{2}}{b\varepsilon_l}\right| \begin{array}{c} \left(-\frac{a_l}{2}, \frac{1}{2}\right), \left(-1-a_l, 1\right) \\ \left(0, 1\right), \left(-a_l, 1\right) \end{array}\right). \tag{14}$$

$$\text{PEP}\left(x_l, \hat{x}_l\right) = \frac{A\Theta_l \sum_{k=0}^{L-l} \binom{L-l}{k}(-1)^k}{b^{a+1}\left[\Gamma\left(a+1\right)\right]^{l+k}} \sum_{n=0}^{\infty} c_n \underbrace{\int_0^{\infty} x^{a+(1+a)(L-l+k)+n} exp\left(-\frac{x}{b}\right) Q\left(\frac{\xi_l\sqrt{\bar{\gamma}_l}x}{2\left|\Delta_l\right|\sqrt{\psi_l\bar{\gamma}_l + d_B^{\alpha}d_{R,l}^{\alpha}}}\right) dx}_{\mathcal{F}_l}. \tag{15}$$

In order to evaluate the PEP, one shall average (7) on all of the possible values of the RV q_l, whose PDF and CDF can be written as [13]:

$$\widetilde{f}_{q_l}\left(x\right) = \frac{x^a}{b^{a+1}\Gamma(a+1)} exp\left(-\frac{x}{b}\right), \tag{8}$$

$$\widetilde{F}_{q_l}\left(x\right) = \frac{\gamma\left(1+a, \frac{x}{b}\right)}{\Gamma(a+1)}, \tag{9}$$

where $a = \frac{k_1^2}{k_2} - 1$, $b = \frac{k_2}{k_1}$, $k_1 = \frac{N\pi}{2}$, $k_2 = 4N\left(1 - \frac{\pi^2}{16}\right)$.

Using order statistics [14], the PDF of the ordered variable is given as

$$f_{q_l}\left(x\right) = \Theta_l\tilde{f}_{q_l}\left(x\right)\left[\tilde{F}_{q_l}\left(x\right)\right]^{l-1}\left[1 - \tilde{F}_{q_l}\left(x\right)\right]^{L-l}, \tag{10}$$

where $\Theta_l = \frac{L!}{(l-1)!(L-l)!}$. By substituting (8) and (9) into (10) and performing some additional some manipulations, one gets

$$f_{q_l}\left(x\right) = \frac{\Theta_l x^a(-1)^k}{b^{a+1}\left[\Gamma\left(a+1\right)\right]^{l+k}} \sum_{k=0}^{L-l} \binom{L-l}{k} exp\left(-\frac{x}{b}\right) \times \left(\gamma\left(1+a, \frac{x}{b}\right)\right)^{L-l+k}. \tag{11}$$

Then, substituting (11) into (7), we can get the uncondition PEP expressions of U_l

$$\text{PEP}\left(x_l, \hat{x}_l\right) = \frac{\Theta_l}{b^{a+1}\left[\Gamma\left(a+1\right)\right]^{l+k}} \sum_{k=0}^{L-l} \binom{L-l}{k}(-1)^k \\ \times \int_0^{\infty} x^a exp\left(-\frac{x}{b}\right) \times \left(\gamma(1+a, \frac{x}{b})\right)^t \\ \times Q\left(\frac{\xi_l\sqrt{\bar{\gamma}_l}x}{2\left|\Delta_l\right|\sqrt{\psi_l\bar{\gamma}_l + d_B^{\alpha}d_{R,l}^{\alpha}}}\right) dx. \tag{12}$$

As seen from (7), the PEP depends on the distance between the transmitted and detected symbols, which is determined by the constellation of the adopted modulation scheme and the channel estimation error variance.

Since the derivations will be highly different under the two scenarios: $\sigma_{el}^2 = 0$ and $\sigma_{el}^2 \neq 0$, so in the following subsections, we will show PEP expressions under the two scenarios.

A. PEP under Scenario 4

Lemma 1: The PEP of U_l under scenario 4, i.e., $\sigma_{e_l} \neq 0$, can be evaluated as (13) which shown at the top of this page. In (13), $\Gamma(\cdot)$ is the complete gamma function, $H_{p,q}^{m,n}(\cdot|\cdot)$ is the bivariate Fox's H-function, $\mathcal{F}_l$ shown at the top of this page as (14), where $a_l = a + (1+a)(L-l+k) + n$,

and

$$\varepsilon_l = \frac{\xi_l\sqrt{\bar{\gamma}_l}}{2\left|\Delta_l\right|\sqrt{\psi_l\bar{\gamma}_l + d_B^{\alpha}d_{R,l}^{\alpha}}}. \tag{16}$$

Proof: By the properties of incomplete gamma functions [12, Eq. (0.314) and Eq.(8.354)], $\gamma(\mu, t) = \sum_{n=0}^{\infty} \frac{(-1)^n t^{\mu+n}}{n!(\mu+n)}$ and $\left(\sum_{k=0}^{\infty} a_k x^k\right)^n = \sum_{k=0}^{\infty} c_k x^k$, where $c_0 = a_0^m$, $c_m = \frac{1}{ma_0}\sum_{k=1}^{m}(kn - m + k)a_k c_{m-k}$, for $m \geq 1$, n is a nature number, substituting $\mu = 1 + a$, $t = \frac{x}{b}$ into (12), $\text{PEP}(x_l, \hat{x}_l)$ can be written as (15), which shown at the top of this page, where $A = \left(\frac{1}{b}\right)^{(1+a)(L-l+k)}$.

Using $Q(x) = \frac{1}{2}\text{erfc}(\frac{x}{\sqrt{2}})$ and [15, Eq. (07.34.03.0228.01)], $\mathcal{F}_l$ in (15) can be expressed as:

$$\mathcal{F}_l = \frac{1}{4\pi j} \oint_{C_z} b_l^{-z}\Gamma(z) dz \int_0^{\infty} x^{-z+a_l}\text{erfc}\left(\frac{\varepsilon x}{\sqrt{2}}\right) dx, \tag{17}$$

where C_z is a complex contour of integration ensuring the convergence of the above Mellin-Barnes integral (i.e., a vertical line separating left poles of the above integrand from the right one (e.g. $-j\infty + \epsilon; j\infty + \epsilon$) with $\epsilon > 0$. Using [16,
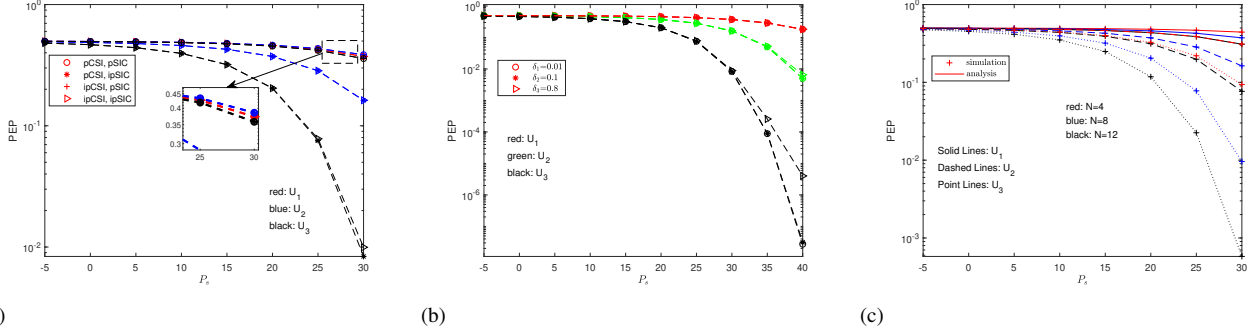
Fig. 1: (a) PEP of three vehicles under all four scenarios versus P_s, (b) PEP versus P_s under different δ, (c) PEP versus P_s with ipCSI and ipSIC under different N

Eq. (4.1.11)] and $\Gamma(x+1) = x\Gamma(x)$, (17) can be expressed as

$$
\mathcal{F}_l = \frac{1}{4\pi j} \oint_{C_z} b_l^{-z} \Gamma(z) \frac{\Gamma\left(-\frac{\alpha z}{2} + \frac{a_l}{2} + 1\right)}{(-\alpha z + a_l + 1)\sqrt{\pi}\left(\frac{\varepsilon}{\sqrt{2}}\right)^{-\alpha z + a_l + 1}} dz
$$

$$
= \frac{1}{4\pi j\sqrt{\pi}} \oint_{C_z} \left(\left(\frac{\sqrt{2}}{\varepsilon}\right)^\alpha b_l\right)^{-z}
$$

$$
\times \frac{\Gamma(z)\Gamma\left(-\frac{\alpha z}{2} + \frac{a_l}{2} + 1\right)\Gamma(-\alpha z + a_l + 2)}{\Gamma(-\alpha z + a_l + 1)} dz.
\tag{18}
$$

Finally, using the definition of Fox's H-function [17], (14) can be easily obtained from (18).

B. PEP under Scenario 2

Scenario 2 corresponds to the ideal conditions that perfect CSI. Let $\sigma_{e_l} = 0$ in (7), we have $\psi_l = 0$ for all users. Under this case, we can have the following modified parameters: $\varepsilon_l = \frac{\xi_l\sqrt{\bar{\gamma}_l}}{2|\Delta_l|\sqrt{d_B^\alpha d_{R,l}^\alpha}}$. Furthermore, the conditional PEP of (7) becomes $\mathrm{PEP}(x_l, \hat{x}_l | q_l) = Q\left(\frac{q_l \xi_l \sqrt{\bar{\gamma}_l}}{2|\Delta_l|\sqrt{d_B^\alpha d_{R,l}^\alpha}}\right)$. The expression of PEP under scenario 2 can be obtained by (13) using the modified ε_l.

C. BER Union Bound

The average of PEP represents an upper bound for the BER, which gives insight into the error rate performance when the BER's form expression is intractable. It is worth noting that the PEP depends on both transmitted and detected symbols of the vehicles. Hence, it should be averaged on all possible values of the transmitted and erroneously detected symbols for a fixed vehicle. Consequently, utilizing the derived PEP expression, the BER union bound of U_l can be evaluated as

$$
P_e \leq \frac{1}{b} \sum_{x_l} \mathrm{Pr}(x_l) \sum_{x_l \neq \hat{x}_l} q(x_l \to \hat{x}_l) \mathrm{PEP}(x_l, \hat{x}_l).
\tag{19}
$$

where b is the number of transmitted bits in x_l, $\mathrm{Pr}(x_l)$ is the probability of transmitting symbol x_l, and $q(x_l \to \hat{x}_l)$ is the number of bit error when choosing $\hat{x}_l$ instead of x_l.

IV. NUMERICAL AND SIMULATION RESULTS

In this section, numerical and Monte Carlo simulation presents the error rate performance of the considered RIS-NOMA system to validate the derived analytical results under both pCSI and ipCSI cases with imperfect SIC process. Without loss of generality, we consider a NOMA system with three vehicles where each vehicle is equipped with a single antenna.

Unless otherwise stated, the transmitted and detected signals are selected randomly from a binary phase shift keying (BPSK) constellation. It is noted that x_l, $\hat{x}_l$ can be either $+1$ or -1 in BPSK modulation, resulting in $|\Delta_l| = 2$. Unless otherwise specified, the simulation parameters are set as shown in TABLE I.

TABLE I: simulation parameters.

Parameter	Value
Noise level	-30 dB
Distance d_B	80 m
Distance $d_{R,1}$, $d_{R,2}$, $d_{R,3}$	150 m, 120 m, 90 m
Path-loss exponent a	2.2
ipCSI impact factor δ	0.8
RIS's RUs N	8
Power allocation ratio α_1, α_2, α_3	1/2, 1/3, 1/6

The PEP performance for three vehicles under the four scenarios is illustrated in Fig. 1 (a). Here, we assume that the ipSIC is implemented by users, i.e., inter-user interference from weaker users that has higher power allocation may exist. It can be seen that the derived analysis, given by (13), is corroborated with the simulation result, where they have shown that the derived analysis and simulation results match perfectly for all of the users over the entire SNR range. The figure shows exciting results in three aspects: (i) The PEP for U_1 under four cases are the same. This is because the first user, i.e., the weakest user, does not implement SIC. Notably, we find that the PEP of U_2 and U_3 under the ipSIC case are significantly lower than that under the pSIC case, which validates the analysis results as elaborated in Remark 1. (ii) We find that ipCSI has a different impact on U_2 and U_3 under ipSIC and pSIC cases. For example, imperfect CSI

significantly affects users' error rate performance when the ipSIC is considered, especially for strong users; when pSIC is considered, the impact of ipCSI is negligible.

Fig. 1 (b) illustrates the error rate performance versus P_s for various values of δ. From the figure, we observe that the user's PEP increase with the increase of δ. This means the greater the number of CSI uncertainties, the worse the user's error rate performance. Moreover, we also find that δ has a different impact on three users, it can be seen that the ipCSI has a more significant effect on strong users, especially at the high P_s.
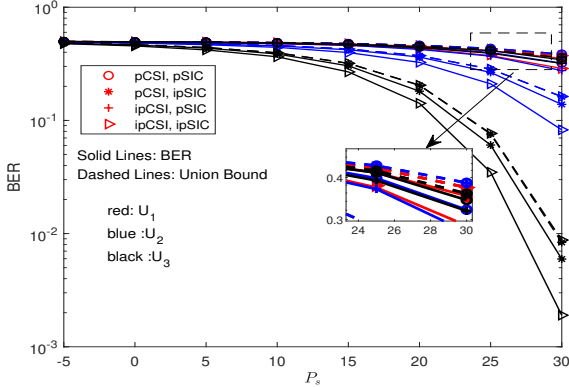

Fig. 2: BER of three users under four scenarios

Fig. 1 (c) shows the PEP performance for the three vehicles, where the analytical and simulation results are presented for $N = 4, 8$ and 12. It can be seen from Fig. 1 (c) that the performance gaps between the three vehicles become large with the increase of RUs. Moreover, we also observe that the users' PEP gaps become larger and larger with the transmit power P_s increases, particularly for U_3, which means that increasing the value of N has a more significant impact on more robust users.

Fig. 2 presents the simulated BER and the derived union bound, where $N = 8$ and the transmitted symbols are randomly chosen from the BPSK constellation. The PEP is averaged over all possible codewords of all users. The figure shows that the near users show strong performance, while the far user has a relatively weak performance.

V. CONCLUSIONS

In this paper, we investigate the joint impact of imperfect channel state information and imperfect SIC on the error rate performance of the RIS-assisted NOMA system. The exact PEP expressions are derived under ideal and non-ideal scenarios. Numerical and analytical results show that ipCSI worsens PEP performance and, with increased N, results in a better error rate performance. Moreover, we found that ipCSI has a different influence on users' PEP under ipSIC and pSIC assumptions. When considering ipSIC, the ipCSI clearly influences PEP, especially for more robust users. When pSIC is taken into account, ipCSI has a negligible impact on the PEP of users.

REFERENCES

[1] L. Zhao, H. Chai, Y. Han, K. Yu, and S. Mumtaz, "A Collaborative V2X Data Correction Method for Road Safety," *IEEE Trans. Rel*, vol. 71, no. 2, pp. 951–962, Jun. 2022.

[2] Y. Zhu, B. Mao, Y. Kawamoto, and N. Kato, "Intelligent reflecting surface-aided vehicular networks toward 6G: Vision, proposal, and future directions," *IEEE Vehicular Technology Magazine*, vol. 16, no. 4, pp. 48–56, 2021.

[3] Y. Chen, Y. Wang, J. Zhang, P. Zhang, and L. Hanzo, "Reconfigurable intelligent surface (ris)-aided vehicular networks: Their protocols, resource allocation, and performance," *IEEE Vehicular Technology Magazine*, vol. 17, no. 2, pp. 26–36, 2022.

[4] W. U. Khan, M. A. Jamshed, E. Lagunas, S. Chatzinotas, X. Li, and B. Ottersten, "Energy Efficiency Optimization for Backscatter Enhanced NOMA Cooperative V2X Communications Under Imperfect CSI," *IEEE Trans. Intell. Transp. Syst.*, pp. 1–12, Jul. 2022.

[5] F. Kara and H. Kaya, "BER performances of downlink and uplink NOMA in the presence of SIC errors over fading channels," *IET Commun.*, vol. 12, no. 15, pp. 1834–1844, Sep. 2018.

[6] L. Bariah, A. Al-Dweik, and S. Muhaidat, "On the Performance of Non-Orthogonal Multiple Access Systems with Imperfect Successive Interference Cancellation," in *IEEE ICC Workshops,* Kansas, May. 2018.

[7] B. Di, L. Song, Y. Li, and Z. Han, "V2X Meets NOMA: Non-Orthogonal Multiple Access for 5G-Enabled Vehicular Networks," *IEEE Wirel Commun*, vol. 24, no. 6, pp. 14–21, Dec. 2017.

[8] X. Li, L. Ma, Y. Xu, and R. Shankaran, "Resource allocation for D2D-based V2X communication with imperfect CSI," *IEEE Internet Things J.*, vol. 7, no. 4, pp. 3545–3558, Apr. 2020.

[9] M. Li, S. Huang, L. Tian, O. Alhussein, and S. Muhaidat, "Error rate performance of NOMA system with full-duplex cooperative relaying," *Physical Communication*, vol. 49, p. 101447, Dec. 2021.

[10] V. C. Thirumavalavan and T. S. Jayaraman, "BER Analysis of Reconfigurable Intelligent Surface Assisted Downlink Power Domain NOMA System," in *2020 International Conference on COMmunication Systems NETworkS (COMSNETS)*, 2020, pp. 519–522.

[11] L. Bariah, S. Muhaidat, P. C. Sofotasios, F. E. Bouanani, O. A. Dobre, and W. Hamouda, "Large Intelligent Surface-Assisted Nonorthogonal Multiple Access for 6G Networks: Performance Analysis," *IEEE Internet of Things Journal*, vol. 8, no. 7, pp. 5129–5140, 2021.

[12] *Table of Integrals, Series, and Products (Seventh Edition)*. Table of Integrals, Series, and Products (Seventh Edition), 2007.

[13] A.-A. A. Boulogeorgos and A. Alexiou, "Performance Analysis of Reconfigurable Intelligent Surface-Assisted Wireless Systems and Comparison With Relaying," *IEEE Access*, vol. 8, pp. 94 463–94 483, 2020.

[14] L. Bariah, S. Muhaidat, and A. Al-Dweik, "Error Probability Analysis of Non-Orthogonal Multiple Access Over Nakagami-m Fading Channels," *IEEE Transactions on Communications*, vol. 67, no. 2, pp. 1586–1599, 2019.

[15] Wolfram Research, *Inc., Mathematica, Version 12.1,* Champaign, IL (2020).

[16] N. E. W. and M. Geller., "A table of integrals of the error functions," *J. Res. Natl. Bureau Stand. B Math. Sci.*, vol. 73B, no. 1, pp. 1–20, 1969.

[17] A. A. Kilbas, *H-transforms: Theory and Applications.* CRC Press, 2004.